BJP BRITISH JOURNAL OF PHARMACOLOGY

BPS BRITISH PHARMACOLOGICAL SOCIETY

British Journal of Pharmacology (2010), 159, 812–819

0007-1188/10
www.brjpharmacol.org

THEMED SECTION: IMAGING IN PHARMACOLOGY

RESEARCH PAPER

Positron emission tomography of [^{18}F]-big endothelin-1 reveals renal excretion but tissue-specific conversion to [^{18}F]-endothelin-1 in lung and liver

Peter Johnström[1], Tim D Fryer[2], Hugh K Richards[3], Janet J Maguire[1], John C Clark[2], John D Pickard[2,3] and Anthony P Davenport[1]

[1]*Clinical Pharmacology Unit,* [2]*Wolfson Brain Imaging Centre and* [3]*Academic Neurosurgery Unit, University of Cambridge, Addenbrooke's Hospital, Cambridge, UK*

Background and purpose: Big endothelin-1 (ET-1) circulates in plasma but does not bind to ET receptors until converted to ET-1 by smooth muscle converting enzymes. We hypothesized that tissue-specific conversion of [^{18}F]-big ET-1 to [^{18}F]-ET-1 could be imaged dynamically *in vivo* within target organs as binding to ET receptors.
Methods: [^{18}F]-big ET-1 conversion imaged *in vivo* following infusion into rats using positron emission tomography (PET).
Key results: [^{18}F]-big ET-1 was rapidly cleared from the circulation ($t_{1/2}$ = 2.9 ± 0.1 min). Whole body microPET images showed highest uptake of radioactivity in three major organs. In lungs and liver, time activity curves peaked within 2.5 min, then plateaued reaching equilibrium after 10 min, with no further decrease after 120 min. Phosphoramidon did not alter half life of [^{18}F]-big ET-1 but uptake was reduced in lung (42%) and liver (45%) after 120 min, consistent with inhibition of enzyme conversion and reduction of ET-1 receptor binding. The ET_A antagonist, FR139317 did not alter half-life of [^{18}F]-big ET-1 ($t_{1/2}$ = 2.5 min) but radioactivity was reduced in all tissues except for kidney consistent with reduction in binding to ET_A receptors. In kidney, however, the peak in radioactivity was higher but time to maximum accumulation was slower (~30 min), which was increased by phosphoramidon, reflecting renal excretion with low conversion and binding to ET receptors.
Conclusions and implications: A major site for conversion was within the vasculature of the lung and liver, whereas uptake in kidney was more complex, reflecting excretion of [^{18}F]-big ET-1 without conversion to ET-1.
British Journal of Pharmacology (2010) **159,** 812–819; doi:10.1111/j.1476-5381.2010.00641.x

This article is part of a themed section on Imaging in Pharmacology. To view the editorial for this themed section visit http://dx.doi.org/10.1111/j.1476-5381.2010.00685.x

Keywords: ET-1; big ET-1; endothelin converting enzyme; positron emission tomography; microPET; [^{18}F]-ET; *in vivo* imaging; phosphoramidon; FR139317

Abbreviations: ET-1, endothelin-1; FR139317, (R)-2-[(R)-2-[(S)-2-[[1-(hexahydro-1H-azepinyl)]carbonyl]amino-4-methylpentanoyl]amino-3-[3-(1-methyl-1H-indoyl)]propionyl] amino-3-(2-pyridyl)propionic acid; PET, positron emission tomography; phosphoramidon, (2S)-2-[[(2S)-2-[[hydroxy-[(2S,3R,4R,5R,6S)-3,4,5-trihydroxy-6-methyloxan-2-yl] oxyphosphoryl] amino]-4-methylpentanoyl]amino]-3-(1H-indol-3-yl) propanoic acid

Introduction

The potent vasoactive peptide endothelin-1 (ET-1) plays an important role in the maintenance of normal vascular tone. It is synthesized in human endothelial cells from its precursor peptide, big ET-1 by a unique cleavage of the Trp^{21}-Val^{22} bond catalysed by ET converting enzymes (ECE) (Davenport and Maguire, 2006). ET-1 is continuously released from the endothelium, causing long-lasting vasoconstriction by stimulation of predominantly ET_A receptors present on the underlying smooth muscle (Russell and Davenport, 1999). In contrast, ET-1 acting on ET_B receptors expressed by the endothelium causes vasodilatation through release of nitric oxide and

Correspondence: Dr Anthony P Davenport, Clinical Pharmacology Unit, University of Cambridge, Addenbrooke's Centre for Clinical Investigation, Level 6, Box 110, Addenbrooke's Hospital, Cambridge CB2 0QQ, UK. E-mail: apd10@medschl.cam.ac.uk
Received 27 July 2009; revised 12 November 2009; accepted 4 December 2009

prostacyclin (de Nucci *et al.*, 1988) counterbalancing the vasoconstriction (Haynes and Webb, 1998). Some big ET-1 escapes conversion by either the intracellular or cell-surface enzymes of the endothelium. Both big ET-1 and the mature peptide, ET-1 are secreted into the medium from human umbilical vein endothelial cells in a ratio of about 1:4 (Plumpton *et al.*, 1994), consistent with the detection of both peptides in human plasma (Suzuki *et al.*, 1990; Matsumoto *et al.*, 1994)

Although Big ET-1 is present in human plasma (Suzuki *et al.*, 1990; Matsumoto *et al.*, 1994) it does not bind to ET receptors at the concentrations circulating in blood and must be converted to ET-1 for receptor activity (Kimura *et al.*, 1989). Infused big ET-1 produces pronounced forearm vasoconstriction with a corresponding increase in plasma ET-1 and the biologically inactive C-terminal fragment. Phosphoramidon, an inhibitor that does not normally cross the plasma membrane, blocks this vasoconstriction, implying local conversion by an ectoenzyme at the site of action (Plumpton *et al.*, 1995). This is most probably vascular smooth muscle ECE, as little or no conversion of big ET-1 to ET-1 has been detected in human blood *in vitro* (Watanabe *et al.*, 1991) and constriction of human isolated blood vessels by big ET-1 persists after endothelial denudation (Mombouli *et al.*, 1993; Maguire *et al.*, 1997). Infusion of big ET-1 into rats (Gardiner *et al.*, 1991; 1993; 1997; Mcmahon *et al.*, 1991; Pollock and Opgenorth, 1991a) causes vasoconstriction, which could be blocked by the neutral endopeptidase/ECE inhibitor, phosphoramidon but not thiorphan, distinguishing this ECE activity from neutral endopeptidase (Pollock and Opgenorth, 1991b). Big ET-1 and ECE are up-regulated in disease (Minamino *et al.*, 1997; Grantham *et al.*, 1998; Maguire and Davenport, 1998). For example, tissue levels of ET-1 and big ET-1 are significantly increased in human vessels with atherosclerotic plaques compared with normal tissue (Bacon *et al.*, 1996). ECE activity is up-regulated in atherosclerotic human coronary arteries resulting in an increased response to big ET-1 (Maguire and Davenport, 1998). These results suggest that significant tissue-specific conversion of big ET-1 may occur in the vasculature and hence add to the detrimental effects caused by increased levels of ET-1 in disease.

Positron emission tomography (PET) is used to image classical transmitter systems *in vivo* although peptides have been less widely studied owing to a lack of suitable ligands. Dedicated tomographs such as microPET have recently been introduced for laboratory animals with spatial resolution to allow the delineation of discrete organs and their larger substructures in rodents (Chatziioannou, 2002; Lewis *et al.*, 2002). We have previously demonstrated using the microPET that binding of [18F]-ET-1 to ET receptors in the rat can be imaged dynamically and that this binding could be blocked when the rats were pretreated with an ET_B selective antagonist (Johnström *et al.*, 2005a). Importantly, binding of [18F]-ET-1 can be imaged using 'tracer' amounts of the peptide, which allows visualization of the receptors without causing vasoconstriction and altering haemodynamics.

We hypothesized that tissue-specific conversion of [18F]-big ET-1 to [18F]-ET-1 could be imaged dynamically *in vivo* within target organs as binding to ET receptors, to provide evidence that big ET-1 could act as a long range signalling hormone. To test our hypothesis, big ET-1 was labelled for the first time with 18F and imaged *in vivo* following infusion into rats. Our aim was to identify the major organs mediating enzymatic conversion of [18F]-big ET-1 to [18F]-ET-1 and whether this could be inhibited by phosphoramidon.

Methods

Animals

All experiments were conducted in accordance with the United Kingdom Animal Scientific Procedures Act, 1986 and complied with guidelines of the local animal ethics committee. Rats were housed with free access to standard rat food and water prior to the experimental procedure. PET experiments were performed in male Sprague-Dawley rats (392 ± 19 g).

Animal preparation

Rats were anaesthetized with 3% isofluorane (Baker Norton, Bristol, UK) vaporized in N_2O/O_2 (0.8/0.4 L per min) and maintained with 2% isofluorane. Body temperature was monitored and maintained in the normal range. A femoral vein was cannulated for administration of [18F]-big ET-1 and preinfusion of phosphoramidon, at a concentration chosen to inhibit the *in vivo* conversion of big ET-1 to ET-1 (Mcmahon *et al.*, 1991; Plumpton *et al.*, 1995) and FR139317 the selective ET_A receptor antagonist (Davenport and Maguire, 2006). The contralateral femoral artery was cannulated for blood sampling and for monitoring blood pressure. As expected injection of [18F]-big ET-1 at these tracer levels did not alter blood pressure compared with baseline. During PET scanning, anaesthesia was reduced to 1.5–2% isofluorane in N_2O/O_2 (0.8/0.4 L per min).

MicroPET imaging

Study design. Dynamic *in vivo* imaging of ECE conversion of [18F]-big ET-1 to [18F]-ET-1 and subsequent binding to ET receptors was studied using microPET. For control experiments using [18F]-big ET-1 alone (n = 3 animals per group according to license PPL80/1439), dynamic scans were performed for up to 2 h. To test the effect of enzyme inhibition, three rats were pretreated with phosphoramidon (10 $mg \cdot kg^{-1}$) immediately prior to injection of [18F]-big ET-1. In one experiment, to confirm that uptake of [18F]-big ET-1 could be blocked by an ET_A selective antagonist, FR139317 (10 $mg \cdot kg^{-1}$) was infused immediately prior to injection of [18F]-big ET-1. Blood samples were collected in Eppendorf tubes at timed intervals.

MicroPET system

Animals were imaged using a microPET P4 scanner (Tai *et al.*, 2001) (Concorde Microsystems, Knoxville, TN, USA). Rats were placed prone on the scanning bed and located in a purpose-built plastic stereotaxic frame. The computer controlled scanning bed was positioned so that the axial field of view (7.8 cm) encompassed the organs of interest.

Acquisition protocol

[18F]-big ET-1 (10.1 ± 0.8 MBq) was administered to the rats as a bolus intravenous injection. A timing window of 10 ns was

used in conjunction with an energy window of 250–750 keV to increase sensitivity. The data were acquired in list mode and were binned into the following time frames starting at the time of tracer administration: 6×5 s, 9×0.5 min, 5×1 min, 15×2 min and then in 5 min frames to the end of the experiment.

Image reconstruction and analysis

All images were reconstructed using the 3D filtered back-projection algorithm (Kinahan and Rogers, 1989) adapted in-house to work with data from the microPET P4 scanner. Corrections were applied to the data during reconstruction as outlined in Johnström *et al.* (2005b). Images were reconstructed into $0.5 \times 0.5 \times 0.5$ mm voxels in an array of $200 \times 200 \times 151$ and a Hanning window cut-off at $0.8 \times$ Nyquist frequency was incorporated into the reconstruction filters.

Regions of interest were delineated for the organs of interest using Analyze (AnalyzeDirect Inc, Lenexa, KS, USA) to construct time-activity curves (Robb *et al.*, 1989). Consistently sized regions were used for all studies and were of sufficient size (≥1.3 mL) that quantification error due to the partial volume effect should not be significant for the resolution of the microPET. Data were corrected for radioactive decay measured in MBq·mL^{-1} and normalized for the dose of injected activity (%ID·g^{-1} tissue or %ID·mL^{-1} blood).

Ex vivo *tissue analysis*

At the end of scanning, animals were killed by intravenous injection of pentobarbitone and organs dissected, weighed and analysed for amount of radioactivity using a gamma counter. These data were quantified by counting a set of ^{18}F standards prepared from the radioligand stock solution. Additionally, cryostat cut sections (30 μm) of tissues were apposed, together with ^{18}F standards prepared from the radioligand stock solution, to a storage phosphor imaging screen (Cyclone, PerkinElmer Life Sciences Ltd, Cambridge, UK). Tissue sections were subsequently stored at –70°C to allow for the decay of ^{18}F and then stained with haematoxylin and eosin or antisera to α-actin as a marker of smooth muscle cells to facilitate histological identification using methods described previously (Davenport and Kuc, 2005). The concentration of radioactivity in weighed blood samples was determined using a well counter.

Statistical analysis

Data are expressed as mean ± SEM. There was no evidence of non-normality and data were analysed by analysis of variance and differences were considered significant at $P < 0.05$.

Peptides and radiolabelling of big ET-1

Big ET-1 and phosphoramidon were obtained from Peptide Institute Inc. (Osaka, Japan). FR139317 was synthesized by Dr A. M. Doherty, Parke-Davis Pharmaceutical Research Division, Ann Arbor, Michigan USA. Phosphoramidon (10 mg·mL^{-1}) and FR139317 (10 mg·mL^{-1}) for injection were dissolved in saline.

Big ET-1 was labelled with ^{18}F in the ε-amino group of Lys^9 by conjugation with the Bolton-Hunter-type reagent *N*-succinimidyl 4-[^{18}F]-fluorobenzoate using the method previously reported for ET-1 (Johnström *et al.*, 2002). Briefly, *N*-succinimidyl 4-[^{18}F]-fluorobenzoate (synthesized from [^{18}F]-fluoride) in anhydrous acetonitrile (20 μL) was added to solution of big ET-1 (100 μL, 1.0 mg·mL^{-1} in sodium bicarbonate (0.04 M)) and left for 30 min at room temperature. The reaction was quenched with HCl (70 μL, 0.3 M) and the mixture was purified using reverse-phase HPLC (Spherisorb ODS2, 5 μ, 4.6×250 mm). [^{18}F]-big ET-1 was eluted using a five-step gradient [50 mM NaH_2PO_4 with 0.1% trifluoroacetic acid (pH 4.0)] : [acetonitrile] 66:34 (v/v) for 5 min, 63:37 for 5 min, 60:40 for 5 min, 57:43 for 5 min and finally 54:46 for 5 min and a flow of 1 mL·min^{-1}. The fraction corresponding to [^{18}F]-big ET-1 was collected (retention time 21–23 min), phosphate buffer (8 mL, 10 mM, pH 7.4) was added and the resulting solution was loaded onto a SepPak C18 Light cartridge. The isolated [^{18}F]-big ET-1 was eluted with ethanol/phosphate buffer (10 mM, pH 7.4) 80:20. Subsequent evaporation of the ethanol using a rotary evaporator and re-dissolving in saline yielded a solution of [^{18}F]-big ET-1 suitable for injection.

Results

Radiolabelling of big ET-1

Big ET-1 was labelled in Lys^9 by conjugation with *N*-succinimidyl 4-[^{18}F]-fluorobenzoate. The radiochemical yield was 12–15% (corrected for decay) and the radiochemical purity of the isolated [^{18}F]-big ET-1 was >95%. The specific activity at injection was 230 ± 21 GBq·μmol^{-1}. The identity of [^{18}F]-big ET-1 was confirmed using HPLC and co-elution with reference (4-fluorobenzoyl)-big ET-1 ([F]-big ET-1) synthesized using the method of Johnström *et al.* (2002). Identity of reference (4-fluorobenzoyl)-big ET-1 was confirmed by mass spectroscopy (MS (m/z) 2203.8 $[M+2H]^{2+}$, 1469.2 $[M+3H]^{3+}$, 1102.7 $[M+4H]^{4+}$).

[^{18}F]-big ET-1 biodistribution in control animals

In control animals, the blood curve constructed over a period of 120 min (Figure 1A), showed that [^{18}F]-big ET-1 was initially rapidly cleared from the circulation with a $t_{1/2} = 2.9 \pm 0.1$ min followed by slower β-phase ($t_{1/2} = 104.6 \pm 8.5$ min).

Whole body microPET images of the rat showed the highest uptake of radioactivity in three major organs: kidney, liver and lung. These were selected for further detailed analysis by constructing time-activity curves over 120 min (Figure 1B–D). The decay-corrected concentration of radioactivity in the lungs peaked within 15 s, followed by an initial rapid decrease, then plateaued and reached equilibrium after 10 min, with no further decrease over the time studied (Figure 1B), consistent with conversion of [^{18}F]-big ET-1 to [^{18}F]-ET-1 and subsequent binding to ET receptors. In liver (Figure 1C) a similar pattern was observed with a slightly later peak of radioactivity after 2.5 min. In marked contrast, in the kidney (Figure 1D), the peak in radioactivity was higher but

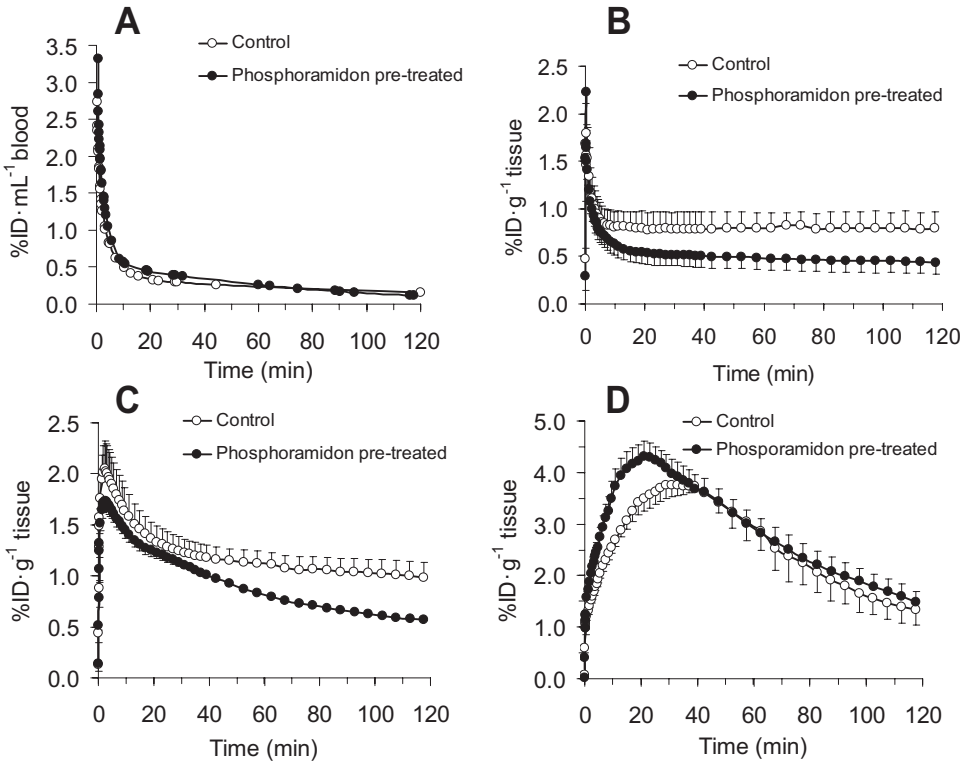

Figure 1 Blood and microPET time-activity curves after [18F]-big ET-1 administration in control, and phosphoramidon pretreated rats: (A) blood curve (B) lung (C) liver and (D) kidney. Activity is shown as % injected dose (%ID) per mL blood or g tissue. By analysis of variance there was a significant reduction in phosphoramidon treated animals in the liver and lung over the complete time-activity curve of 120 min ($P < 0.05$) and in the kidney a significant increase from 1-40 min ($P < 0.05$). ET-1, endothelin-1; PET, positron emission tomography.

time to maximum accumulation was slower (about 30 min), followed by an exponential decline with a $t_{1/2}$ = 59.7 ± 2.8 min.

At the end of the 120 min scanning period, organs were removed for *ex vivo* measurement of radioactivity using a gamma counter (Figure 2), confirming high levels of activity in lung, liver and kidney with lower but detectable levels of uptake in three further organs: heart, muscle and the highly vascular spleen. As expected from previous studies imaging ET receptors *in vivo* following infusion of [18F]-ET-1 in the periphery which did not cross the blood-brain barrier (Johnström *et al.*, 2005a), there was no detectable radioactivity in the brain.

Effect of enzyme inhibition with phosphoramidon

In the blood activity curves (Figure 1), the half-life for [18F]-big ET-1 when the rats where pretreated with phosphoramidon (10 mg·kg^{-1}, $t_{1/2}$ = 2.4 ± 0.1 min, Figure 1A) was similar to the controls. However, uptake of [18F]-big ET-1 in lung and liver (Figure 1B,C) was significantly reduced over the time period of 120 min measured by microPET imaging and in all tissues analysed *ex vivo* (Figure 2) at the end of the experiments, with the exception of kidney and muscle. Analysis of the images showed in the lung and liver that pretreatment resulted in a reduction in uptake by 42% and 45%, respectively, after 120 min. Furthermore the late kinetic data suggests a change

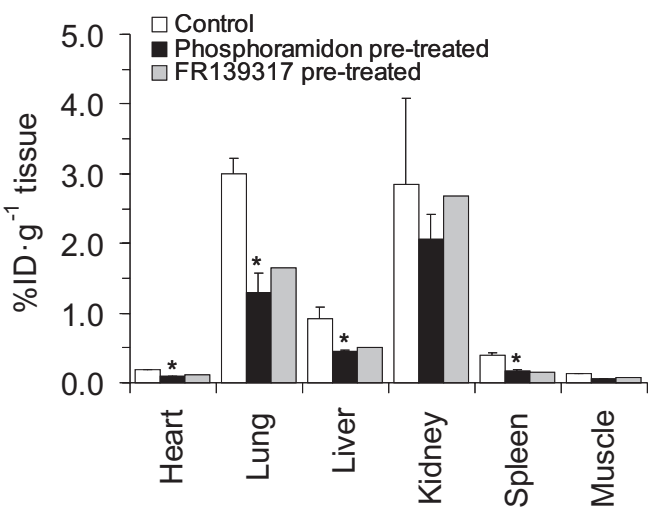

Figure 2 Concentration of radioactivity following excision of tissues at the end of experiment following [18F]-big ET-1 administration in control (n = 3) and after pretreatment with either phosphoramidon (n = 3) rats or FR139317 (n = 1). Phosphoramidon significantly reduced ($P < 0.05$) radioactivity in heart, lung, liver and spleen consistent with inhibition of conversion of [18F]-big ET-1 to [18F]-ET-1. In a single experiment, the ET_A selective antagonist FR139317 reduced radioactivity in the same tissues, consistent with blocking [18F]-ET-1 binding to ET_A receptors. ET-1, endothelin-1.

from steady-state to a slow wash-out phase in lung ($t_{1/2}$ = 297.9 ± 32.1 min) and in the liver ($t_{1/2}$ = 131.9 ± 3.7 min).

In marked contrast in kidney, the amount of radioactivity increased significantly from 1 to 40 min in the presence of phosphoramidon but it did not change the shape of the subsequent time activity curve (Figure 1D) with a comparable exponential decline ($t_{1/2}$ = 62.3 ± 2.6 min). There was no significant change in the level of accumulated radioactivity at the end of the experiment compared with the control (Figures 1 and 2).

Effect of ET_A receptor blockade with FR139317

In a single experiment, pretreatment with the ET_A selective antagonist, FR139317 did not alter the half-life of [18F]-big ET-1 ($t_{1/2}$ = 2.5 min) in the blood whereas a reduction in uptake of radioactivity in the tissue comparable to that in the phosphoramidon pretreated rats was observed in all tissues except for kidney at the end of 120 min, consistent with reduction in binding to ET_A receptors. In agreement with the control and the phosphoramidon results, there was no change in the kidney at end of 120 min consistent with the signal being dominated by excretion of radioactivity (Figure 2).

Comparison of microPET images and ex vivo *autoradiography*

The distribution of radioactivity was examined in more detail by comparing *in vivo* microPET images with *ex vivo* autoradiographical sections of the liver, lung and kidney. After 120 min the reconstructed microPET images in the liver and lung revealed a discrete pattern of high levels of radioactivity suggesting binding to the vasculature (Figure 3A,C). This distribution was observed in *ex vivo* tissue sections of liver and lung, confirming that the radioactivity was localized to the lung vasculature (Figure 3B,D) identified by comparison with the sections stained for the smooth muscle marker, α-actin or haematoxylin and eosin. High levels of radioactivity correlated with larger blood vessels although some radioactivity may be associated with capillary beds. A similar distribution pattern has previously been observed in animals treated with BQ788 to block ET_B receptors in order to visualize binding of [18F]-ET-1 to the ET_A sub-type using microPET imaging (Figure 3E) and autoradiography (Figure 3F) (Johnström *et al.*, 2005a).

In the kidney, microPET images reveal initial high accumulation of radioactivity in the cortex after 15 min, corresponding to the peak of radioactivity measured in the time activity curve with subsequent redistribution with time to the papilla, a pattern consistent with excretion of radioactivity (Figure 4A–D). The autoradiographical images of kidney sections removed at the end of the experiment showed a similar distribution with most of the radioactivity redistributed to the renal papilla (Figure 4E), with some low levels of radioactivity localized to the vasculature of the cortex after 120 min.

A comparable localization of radioactivity to blood vessels was observed in autoradiography of *ex vivo* tissue sections of heart and spleen although levels were too low to allow visualization with microPET (Figure 5A,B).

Discussion

Our results showed that following infusion of [18F]-big ET-1 into anaesthetized rats, the peptide is rapidly cleared from the

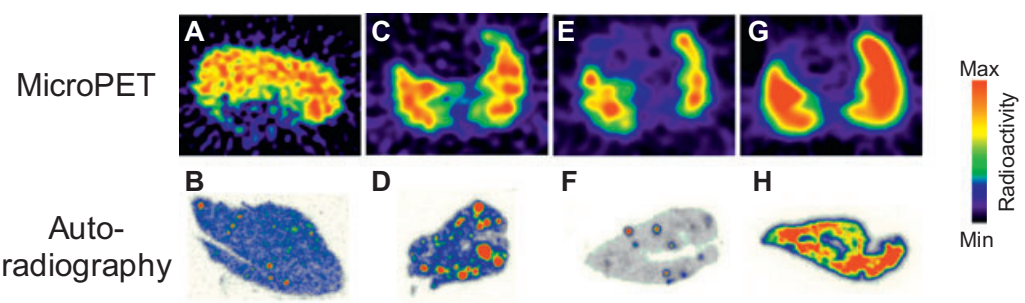

Figure 3 MicroPET images showing localized distribution of radioactivity in liver (A) and lung (C) after [18F]-big ET-1 administration in control rats. This was corroborated by autoradiography of *ex vivo* tissue sections of liver (B) and lung (D) confirming that the radioactivity was localized to the vasculature. For comparison, data from Johnström *et al.* (2005a) are shown where a comparable localized distribution in the lung was observed when the ET_B receptor had been blocked using the ET_B antagonist BQ788 prior to infusion of [18F]-ET-1: (E) Micropet image of the lung and (F) corresponding autoradiography of *ex vivo* tissue section. The Micropet image of [18F]-ET-1 binding in the control rat lung is shown in (G) together with the corresponding autoradiography of *ex vivo* tissue section (H). ET-1, endothelin-1; PET, positron emission tomography.

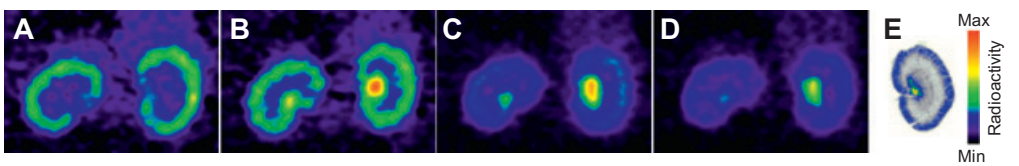

Figure 4 MicroPET images showing the distribution of radioactivity in the kidney as a function of time: (A–D) 15, 40, 65 and 75 min post big-ET-1 injection. The pattern over time is dominated by that expected for excretion rather than binding of the radioligand to receptors. *Ex vivo* autoradiography of kidney sections at end of the imaging experiment shows that most of the radioactivity is in the renal papilla with low levels of radioactivity localized to the vasculature of the cortex (E). ET-1, endothelin-1; PET, positron emission tomography.

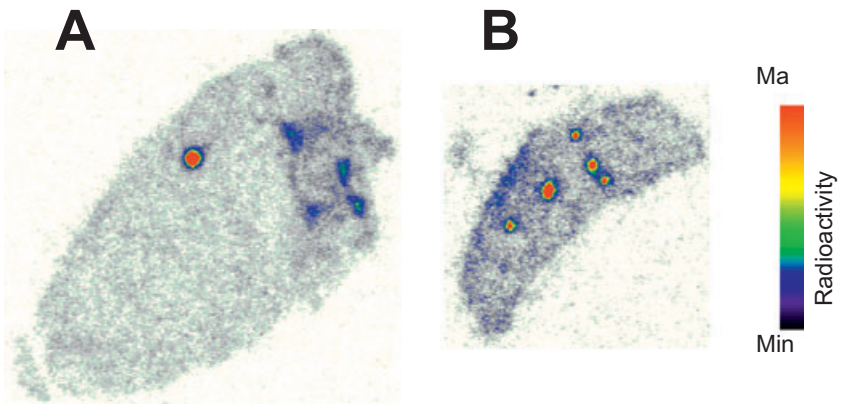

Figure 5 *Ex vivo* autoradiography following PET imaging showing localization of radioactivity to the vasculature in tissue sections of heart (A) and spleen (B). PET, positron emission tomography.

circulation. Major organs for accumulation of radioactivity were identified as the lung, liver and kidney, visualized by dynamic PET imaging, with lower but detectable levels in the heart, spleen and muscle measured by gamma counting of excised organs 2 h after [^{18}F]-big ET-1 administration. Dynamic PET data in the lungs revealed an initial rapid clearance of [^{18}F]-big ET-1, which then levelled out and reached a steady state after 10 min, similar to that previously observed with [^{18}F]-ET-1 infused into rats, consistent with binding to ET receptors (Johnström *et al.*, 2005a). For liver, the steady state was reached later at ~30–40 min which may reflect differences in ECE activity in these organs.

Big ET-1 has no affinity for the ET receptor at the tracer concentrations used in this study and the cleavage of this peptide to ET-1 is essential for receptor binding (Kimura *et al.*, 1989). We have previously shown that the peptide labelling technique used in this study results in conjugation of a [^{18}F]-fluorobenzoyl group with the ε-amino group of Lys^{9} of ET-1 (Johnström *et al.*, 2002). [^{18}F]-ET-1 labelled in this position retains subnanomolar affinity for ET receptors and has pharmacokinetic and pharmacodynamic properties allowing dynamic imaging of ET receptors *in vivo* using PET (Johnström *et al.*, 2005a). It has been shown that the His^{27}-Gly^{34} sequence in big ET-1 is important for enzyme recognition and conversion to ET-1 (Okada *et al.*, 1991; 1993; Brooks and Ergul, 1998). Our strategy avoids labelling within this His^{27}-Gly^{34} region, permitting both enzymic cleavage and formation of [^{18}F]-ET-1.

Metabolic degradation of big ET-1 to longer or shorter amino acid sequences than the optimal ET-1 (1–21) will result in peptides with little or no affinity for ET receptors (Kimura *et al.*, 1988; 1989) suggesting that our data reflects conversion of [^{18}F]-big ET-1 to [^{18}F]-ET-1 and subsequent binding to ET receptors. This is supported by the seven-fold increase in the initial half-life for [^{18}F]-big ET-1 in the blood, compared with the half-life of [^{18}F]-ET-1 (0.43 min) previously measured in the rat (Johnström *et al.*, 2005a). Furthermore, pretreatment with phosphoramidon resulted in a reduction in the level of uptake and a more rapid clearance of radioactivity from lung over time in agreement with inhibition of enzyme conversion and reduction of ET-1 binding to ET receptors. These results are in concordance with previous studies where phosphoramidon treatment blocked *in vivo* vasoconstrictor actions of infused big ET-1 in the rat (Gardiner *et al.*, 1991; Mcmahon *et al.*, 1991; Pollock and Opgenorth, 1991a) and human (Plumpton *et al.*, 1995). Importantly, Pollock and Opgenorth (1991a) demonstrated that phophoramidon had no effect on the vasoconstrictor actions of ET-1 infused *in vivo,* thus excluding the possibility that phosphoramidon blocked binding of ET-1 to its receptor rather than inhibiting conversion of big ET-1. The concentration of phosphoramidon used in this study was chosen as this dose has previously been shown to inhibit *in vivo* constrictor actions of big ET-1 in rats by about 60% (Mcmahon *et al.*, 1991) In agreement, the magnitude of inhibition by phosphoramidon ranging from 51% for liver to 63% for muscle was similar for all tissues studied with the exception of kidney.

Several lines of evidence suggest the site of conversion that we measure is most likely to be ECE present on the smooth muscle, followed by [^{18}F]-ET-1 binding immediately to receptors, particularly the ET_A sub-type that predominates on the smooth muscle. Little or no conversion of big-ET-1 to the mature peptide is thought to occur in the blood (Watanabe *et al.*, 1991) and phosphoramidon had no effect on the blood curve in this study. We have previously shown that most of the endothelial cell ECE activity (~85%) is within the cytoplasm and not the cell surface (Davenport *et al.*, 1998) and as phosphoramidon does not cross the plasma membrane, significant conversion of [^{18}F]-big ET-1 is unlikely to be effected by the endothelium. Furthermore, isolated vessels denuded of endothelium rapidly convert big ET-1 to cause vasoconstriction, corresponding to formation of the mature peptide in the organ bath and this activity is significantly increased in vessels with atherosclerotic lesions (Maguire and Davenport, 1998). Our results with the ET_A receptor selective antagonist FR139317 support the formation of [^{18}F]-ET-1 and binding to the ET_A receptor subtype (nomenclature follows Alexander *et al.*, 2009). MicroPET images and the higher resolution afforded by autoradiography visualized high levels of binding to the vasculature in all tissues examined.

Our results for the accumulation of [^{18}F]-big ET-1 in the kidney are intriguing in that the peak in radioactivity after 20 min in the cortex is the highest for all organs imaged. The magnitude of the peak is further increased in the presence of

phosphoramidon, consistent with the reduction in tissue-specific conversion of [18F]-big ET-1 to [18F]-ET-1 that we measured in other organs and a subsequent increase in excretion of [18F]-big ET-1. After 20 min, radioactivity is redistributed to the medulla which is unchanged by phosphoramidon. Although autoradiography revealed very low levels of binding to the renal vasculature this pattern is consistent with most of the radioactivity being excreted. This may be either unconverted [18F]-big ET-1 or much shorter peptide fragments with little receptor binding action.

Previously we have shown that infusion of [18F]-ET-1 into the rat results in rapid binding to ET receptors in the kidney which can be blocked by antagonists (Johnström *et al*., 2005a) at densities comparable to lungs and liver. Thus if a similar high level of local conversion of [18F]-big ET-1 as that seen in lungs and liver had occurred within the kidney, we would have expected to see greater evidence for this in the kinetic data and *ex vivo* autoradiography at the end of the experiment. Big ET-1 has been identified and found to be more abundant than ET-1 in human urine by specific ELISA HPLC (Matsumoto *et al*., 1994) and Naruse *et al*. (1991) showed by HPLC that urinary levels are increased in patients with cardiovascular disease supporting the hypothesis that the kidney may have a previously unsuspected function to remove a significant component of big ET-1 from the circulation. Some binding was visualized to the renal vasculature which is consistent with previous *in vivo* studies in rats where low doses of big ET-1 (0.1 nmol·kg^{-1}) had no effect on renal haemodynamics whereas vasoconstriction was detected in other vascular beds measured (hindquarters and mesentery) (Gardiner *et al*., 1991).

Our results show that the hepatic and the pulmonary vasculatures are a major site for [18F]-big ET-1 conversion and binding to ET receptors in the rat. It is not yet clear whether the results have clinical significance. However, in pulmonary arterial hypertension which is associated with increases in pulmonary vascular resistance, the ET system is up-regulated and the mixed ET_A/ET_B receptor antagonist, bosentan is used to treat this condition. The source of increased ET-1 is not established although enhanced production or reduced ET_B clearance have been proposed (Dupuis *et al*., 1996; Dupuis *et al*., 1998). Our results suggest a third possibility, of increased conversion of big ET-1 within the target vasculature. Similarly, ET levels are higher in patients with cirrhosis of the liver (Martinet *et al*., 1996) and conversion of big ET-1 by the hepatic circulation may contribute to portal hypertension (Martinet *et al*., 1996). Lower but detectable conversion in the heart could also have pathophysiological actions particularly under conditions where smooth muscle ECE activity is increased, for example in atherosclerosis (Minamino *et al*., 1997; Grantham *et al*., 1998; Maguire and Davenport, 1998), that might promote vasospasm. The renal vasculature is very sensitive to the constrictor actions of ET-1 but surprisingly our results suggest most of the injected radioactivity is being excreted without conversion to ET-1 within the vasculature. Finally, specific inhibitors of ECE are being developed (Jeng *et al*., 2002; Jeng, 2003) to attenuate the proteolytic synthesis of ET-1. Our results suggest under conditions of ECE inhibition, renal excretion may be an important route for removal of big ET-1.

Acknowledgements

We thank Mrs Rhoda Kuc, Miss Morgan Alexander, Dr Olivier Barret and Mr Paul Burke for technical support. This work was supported by grants from the British Heart Foundation, the Medical Research Council and for the microPET a JREI grant from HEFCE and Merck Sharpe & Dohme, Ltd.

Conflicts of interest

None.

References

Alexander SPH, Mathie A, Peters JA (2009). Guide to Receptors and Channels (GRAC), 4th edn. *Br J Pharmacol* **158** (Suppl. 1): S1–S254.

Bacon CR, Cary NRB, Davenport AP (1996). Endothelin peptide and receptors in human atherosclerotic coronary artery and aorta. *Circ Res* **79**: 794–801.

Brooks C, Ergul A (1998). Identification of amino acid residues in the C-terminal tail of big endothelin-1 involved in processing to endothelin-1. *J Mol Endocrinol* **21**: 307–315.

Chatziioannou AF (2002). Molecular imaging of small animals with dedicated PET tomographs. *Eur J Nucl Med Mol Imaging* **29**: 98–114.

Davenport AP, Kuc RE (2005). Immunocytochemical localization of receptors using light and confocal microscopy with application to the phenotypic characterization of knock-out mice. *Methods Mol Biol* **306**: 155–172.

Davenport AP, Kuc RE, Mockridge JW (1998). Endothelin-converting enzyme in the human vasculature: evidence for differential conversion of big endothelin-3 by endothelial and smooth-muscle cells. *J Cardiovasc Pharmacol* **31** (Suppl. 1): S1–S3.

Davenport AP, Maguire JJ (2006). Endothelin. *Handb Exp Pharmacol* **176**: 295–329.

Dupuis J, Cernacek P, Tardif JC, Stewart DJ, Gosselin G, Dyrda I *et al*. (1998). Reduced pulmonary clearance of endothelin-1 in pulmonary hypertension. *Am Heart J* **135**: 614–620.

Dupuis J, Stewart DJ, Cernacek P, Gosselin G (1996). Human pulmonary circulation is an important site for both clearance and production of endothelin-1. *Circulation* **94**: 1578–1584.

Gardiner SM, Compton AM, Kemp PA, Bennett T (1991). The effects of phosphoramidon on the regional haemodynamic responses to human proendothelin [1-38] in conscious rats. *Br J Pharmacol* **103**: 2009–2015.

Gardiner SM, Kemp PA, Bennett T (1993). Regional haemodynamic responses to intravenous and intraarterial endothelin-1 and big endothelin-1 in conscious rats. *Br J Pharmacol* **110**: 1532–1536.

Gardiner SM, Kemp PA, Brunner-Ferber F, Bennett T (1997). Effects of the dual metallopeptidase inhibitor, MDL 100,240, on regional haemodynamic responses to vasoactive peptides in conscious rats. *Br J Pharmacol* **122**: 1687–1693.

Grantham JA, Grantham JA, Schirger JA, Williamson EE, Heublein DM, Wennberg PW *et al*. (1998). Enhanced endothelin-converting enzyme immunoreactivity in early atherosclerosis. *J Cardiovasc Pharmacol* **31** (Suppl. 1): S22–S26.

Haynes WG, Webb DJ (1998). Endothelin as a regulator of cardiovascular function in health and disease. *J Hypertens* **16**: 1081–1098.

Jeng AY (2003). Utility of endothelin-converting enzyme inhibitors for the treatment of cardiovascular diseases. *Curr Opin Investig Drugs* **4**: 1076–1081.

Jeng AY, Mulder P, Kwan AL, Battistini B (2002). Nonpeptidic endothelin-converting enzyme inhibitors and their potential therapeutic applications. *Can J Physiol Pharmacol* **80**: 440–449.

Johnström P, Fryer TD, Richards HK, Barret O, Davenport AP (2005b). Dynamic in vivo imaging of receptors in small animals using positron emission tomography. *Methods Mol Biol* **306**: 217–232.

Johnström P, Fryer TD, Richards HK, Harris NG, Barret O, Clark JC *et al*. (2005a). Positron emission tomography using 18F-labelled endothelin-1 reveals prevention of binding to cardiac receptors owing to tissue-specific clearance by ET_B receptors in vivo. *Br J Pharmacol* **144**: 115–122.

Johnström P, Harris NG, Fryer TD, Barret O, Clark JC, Pickard JD *et al*. (2002). 18F-Endothelin-1, a positron emission tomography (PET) radioligand for the endothelin receptor system: radiosynthesis and in vivo imaging using microPET. *Clin Sci (Lond)* **103** (Suppl. 48): 4S–8S.

Kimura S, Kasuya Y, Sawamura T, Shinimi O, Sugita Y, Yanagisawa M *et al*. (1989). Conversion of big endothelin-1-21-residue endothelin-1 is essential for expression of full vasoconstrictor activity: structure-activity relationships of big endothelin-1. *J Cardiovasc Pharmacol* **13** (Suppl. 5): S5–S7.

Kimura S, Kasuya Y, Sawamura T, Shinmi O, Sugita Y *et al*. (1988). Structure-activity relationships of endothelin: importance of the C-terminal moiety. *Biochem Biophys Res Commun* **156**: 1182–1186.

Kinahan PE, Rogers JG (1989). Analytic 3D image-reconstruction using all detected events. *IEEE Trans Nucl Sci* **36**: 964–968.

Lewis JS, Achilefu S, Garbow JR, Laforest R, Welch MJ (2002). Small animal imaging. current technology and perspectives for oncological imaging. *Eur J Cancer* **38**: 2173–2188.

McMahon EG, Palomo MA, Moore WM, McDonald JF, Stern MK (1991). Phosphoramidon blocks the pressor activity of porcine big endothelin-1-(1-39) in vivo and conversion of big endothelin-1-(1-39) to endothelin-1-(1-21) in vitro. *Proc Natl Acad Sci USA* **88**: 703–707.

Maguire JJ, Davenport AP (1998). Increased response to big endothelin-1 in atherosclerotic human coronary artery: functional evidence for up-regulation of endothelin-converting enzyme activity in disease. *Br J Pharmacol* **125**: 238–240.

Maguire JJ, Johnson CM, Mockridge JW, Davenport AP (1997). Endothelin converting enzyme (ECE) activity in human vascular smooth muscle. *Br J Pharmacol* **122**: 1647–1654.

Martinet JP, Legault L, Cernacek P, Roy L, Dufresne MP, Spahr L *et al*. (1996). Changes in plasma endothelin-1 and Big endothelin-1 induced by transjugular intrahepatic portosystemic shunts in patients with cirrhosis and refractory ascites. *J Hepatol* **25**: 700–706.

Matsumoto H, Suzuki N, Kitada C, Fujino M (1994). Endothelin family peptides in human plasma and urine: their molecular forms and concentrations. *Peptides* **15**: 505–510.

Minamino T, Kurihara H, Takahashi M, Shimada K, Maemura K, Oda H *et al*. (1997). Endothelin-converting enzyme expression in the rat vascular injury model and human coronary atherosclerosis. *Circulation* **95**: 221–230.

Mombouli JV, Le SQ, Wasserstrum N, Vanhoutte PM (1993). Endothelins 1 and 3 and big endothelin-1 contract isolated human placental veins. *J Cardiovasc Pharmacol* **22** (Suppl. 8): S278–S281.

Naruse K, Naruse M, Watanabe Y, Yoshihara I, Ohsumi K, Horiuchi J *et al*. (1991). Molecular form of immunoreactive endothelin in plasma and urine of normal subjects and patients with various disease states. *J Cardiovasc Pharmacol* **17** (Suppl. 7): S506–S508.

de Nucci G, Thomas R, D'Orleans-Juste P, Antunes E, Walder C, Warner TD *et al*. (1988). Pressor effects of circulating endothelin are limited by its removal in the pulmonary circulation and by the release of prostacyclin and endothelium-derived relaxing factor. *Proc Natl Acad Sci USA* **185**: 9797–9800.

Okada K, Arai Y, Hata M, Matsuyama K, Yano M (1993). Big endothelin-1 structure important for specific processing by endothelin-converting enzyme of bovine endothelial cells. *Eur J Biochem* **218**: 493–498.

Okada K, Takada J, Arai Y, Matsuyama K, Yano M (1991). Importance of the C-terminal region of big endothelin-1 for specific conversion by phosphoramidon-sensitive endothelin converting enzyme. *Biochem Biophys Res Commun* **180**: 1019–1023.

Plumpton C, Haynes WG, Webb DJ, Davenport AP (1995). Phosphoramidon inhibition of the in vivo conversion of big endothelin-1 to endothelin-1 in the human forearm. *Br J Pharmacol* **116**: 1821–1828.

Plumpton C, Kalinka S, Martin RC, Horton JK, Davenport AP (1994). Effects of phosphoramidon and pepstatin A on the secretion of endothelin-1 and big endothelin-1 by human umbilical vein endothelial cells: measurement by two-site enzyme-linked immunosorbent assays. *Clin Sci (Lond)* **87**: 245–251.

Pollock DM, Opgenorth TJ (1991a). Comparison of the hemodynamic effects of endothelin-1 and big endothelin-1 in the rat. *Biochem Biophys Res Commun* **179**: 1122–1126.

Pollock DM, Opgenorth TJ (1991b). Evidence for metalloprotease involvement in the in vivo effects of big endothelin 1. *Am J Physiol* **261**: R257–R263.

Robb RA, Hanson DP, Karwoski RA, Larson AG, Workman EL, Stacy MC (1989). Analyze: a comprehensive, operator-interactive software package for multidimensional medical image display and analysis. *Comput Med Imaging Graph* **13**: 433–454.

Russell FD, Davenport AP (1999). Secretory pathways in endothelin synthesis. *Br J Pharmacol* **126**: 391–398.

Suzuki N, Matsumoto H, Kitada C, Kimura S, Miyauchi T, Fujino M (1990). A sandwich-type enzyme immunoassay to detect immunoreactive big-endothelin-1 in plasma. *J Immunol Methods* **127**: 165–170.

Tai YC, Ruangma A, Rowland D, Siegel S, Newport DF, Chow PL *et al*. (2001). Performance evaluation of the microPET P4: a PET system dedicated to animal imaging. *Phys Med Biol* **46**: 1845–1862.

Watanabe Y, Naruse M, Monzen C, Naruse K, Ohsumi K, Horiuchi J *et al*. (1991). Is big endothelin converted to endothelin-1 in circulating blood? *J Cardiovasc Pharmacol* **17** (Suppl. 7): S503–S505.